Polar Geosci., **11**, 61–75, 1998

SYSTEMATIC DEVIATIONS OF EARTHQUAKE SLIP VECTORS FROM NUVEL1 AT THE AUSTRALIA–ANTARCTICA AND PACIFIC–ANTARCTICA PLATE BOUNDARIES

Atsuki KUBO*, Yoshifumi NOGI and Katsutada KAMINUMA

National Institute of Polar Research, Kaga 1-chome, Itabashi-ku, Tokyo 173-8515

Abstract: Systematic deviations of slip vectors from predictions based on plate motion model (NUVEL1 and GPS observation) are discussed at the circum Antarctic plate boundaries. Earthquakes with seismic moments larger than $10^{24.9}$ dyne·cm are considered in the analysis. Results show clear systematic deviations at the eastern end of the Australia–Antarctica plate boundary and the eastern part of the Pacific–Antarctica plate boundary. Around the eastern end of the Australia–Antarctica plate boundary, slip vectors deviate from the relative plate motions predicted by either NUVEL1 or GPS observations. Slip vector deviations due to 1) unrecognized microplate hypothesis near the plate boundary and 2) relative motion between East and West Antarctica are inconsistent with stress and slip direction of intraplate earthquake in the Antarctic plate. Deformation of the plate boundary related to reorganization near the triple junction of the Pacific–Australia–Antarctic plates is the most plausible explanation for the slip vector deviations. In contrast, the cause of slip vector deviations observed around the eastern part of the Pacific–Antarctica remains unclear suggesting complicated origins.

key words: slip vector, relative plate motion, Antarctica, microplate, plate boundary reorganization

1. Introduction

An earthquake slip vector indicates the direction of relative motion between two adjacent plates. Many researchers have tried to construct global plate motion models using 1) slip vectors of earthquakes, 2) strikes of the fracture zones and 3) seafloor spreading rates (*e.g.* MINSTER *et al.*, 1974; MINSTER and JORDAN, 1978; CHASE, 1978; DEMETS *et al.*, 1990). A strike of the fracture zone is also used as a direction of plate motion to construct plate motion model. However, the spreading rate and strike of a fracture zone reflect the plate motion direction averaged over about 3 my, while the temporal resolution of slip vectors and geodetic measurements is less than 100 y. These are shorter than those of fracture zones and spreading rates. We focus on the present instantaneous motions using earthquake slip vectors and geodetic results.

Recently, satellite geodetic techniques have come to be used for the direct determination of plate motions (*e.g.* ARGUS and HEFLIN, 1995; HEKI, 1996; LARSON *et al.*, 1997). Motions calculated from plate models, such as NUVEL1, are consistent with those

* Present address: Earthquake Research Institute, University of Tokyo, 1–1, Yayoi 1-chome, Bunkyo-ku, Tokyo 113-0032.

determined by geodetic measurements. This implies the validity of plate tectonics. However, small differences between motions predicted by a plate model and those obtained by geodetic studies are important to discuss the detailed dynamics of plate motion. Slip vectors of earthquakes and strikes of fracture zones reflect not only relative motions of rigid plates but also deformation associated with 1) plate boundary reorganization and 2) motion of microplates near the plate boundary. Because the results of satellite geodetic measurements do not include deformations of plate boundaries except for islands near the plate boundary, comparison of slip vector directions with geodetic measurements is useful to detect deformation of the plate boundary.

2. Tectonic Setting of the Antarctic Plate

The Antarctic plate is enclosed by six plates including the Scotia plate and enclosed by ridges and transform faults (see Fig. 1). The spreading rates of ridges obtained by the NUVEL1 model ranges from 1 to 10 cm/y. Spreading rates faster than 4 cm/y have been estimated for the relative motion between Australia (AUS), Pacific (PAC), and Nazca (NAZ) plates, and the Antarctic plate (ANT) in the range of 70° E–280° E (or 80° W). In contrast, spreading rates slower than 4 cm/y have been determined for the Scotia (SCO), South America (SAM) and Africa (AFR) plates in the range from 60° E to 280° E (or 80° W) (Fig. 1).

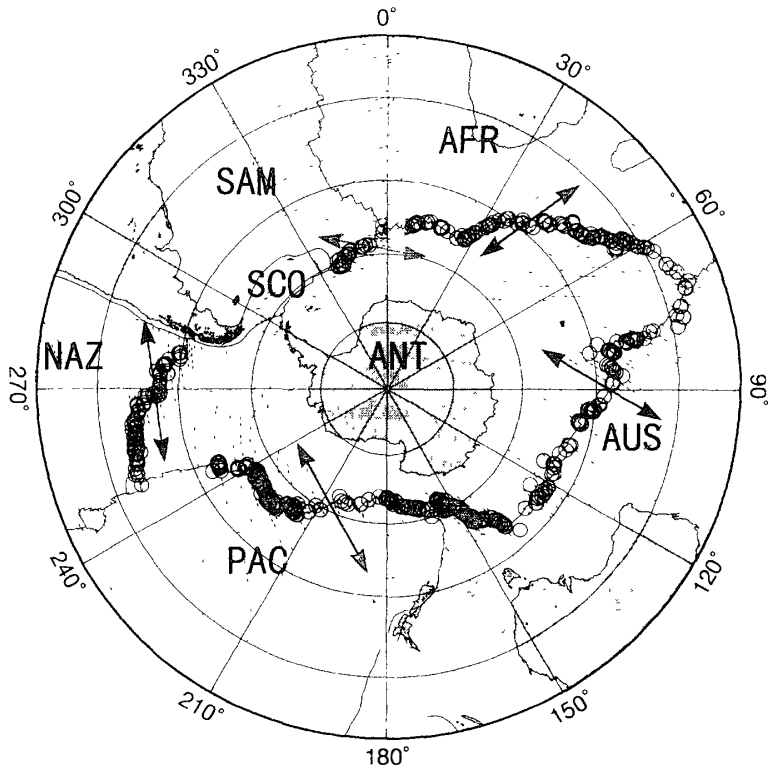

Fig. 1. Plate configuration and epicenters of the circum Antarctic area. Solid and dashed lines indicate plate boundaries and fracture zones, respectively. Arrows are typical directions of relative plate motions. Open circles show epicenters used in this study.

The continent of Antarctica is divided into two provinces by the Transantarctic Mountains. East Antarctica is a stable and Cambrian or older tectonic province; West Antarctica is a tectonically active region and shows younger geological features (DALZIEL, 1992). This contrast has also been detected in the seismic structure of the lithosphere beneath the continent (ROULT *et al.*, 1994). Moreover relative motions between East and West Antarctica or within West Antarctica since Late Cretaceous was proposed by reconstruction study (MOLNAR *et al.*, 1975). Therefore, a possibility of present motion between East and West Antarctica should be considered in this study.

3. Data and Method

Slip vectors of 693 earthquakes which took place along the circum Antarctic plate boundaries during the period 1977–1996 are determined using Harvard Centroid Moment Tensor solutions (HCMT: DZIEWONSKI *et al.*, 1981; DZIEWONSKI and WOODHOUSE, 1983) to examine if any systematic deviations of slip vectors from those predicted by NUVEL1 (DEMETS *et al.*, 1990) are observed. Seismic moments of earthquakes used in this study ranges from $10^{23.3}$ to $10^{26.8}$ dyne·cm. Because tectonic setting of the Scotia plate, which includes subduction zones, involves complex tectonic interactions among circum-Antarctic plates six (PELAYO and WIENS, 1989), results of the slip vectors for the SCO–ANT plates are excluded.

The spatial geometry of a earthquake fault and the definition of a slip vector are illustrated in Fig. 2. The strike of the fault is denoted as ϕ, the dip of the fault δ, the rake angle as λ, ψ is the angle measured on the horizontal plane between strike and horizontally projected direction of slip vector. The slip direction of the earthquake is θ_{slip} and the predicted direction of the relative motion model is θ_{model}. The slip vector deviation is defined as $\delta\theta=\theta_{slip}-\theta_{model}$. The slip vector for each earthquake is determined as follows.

1) The value θ_{model} is calculated based on NUVEL1 for each earthquake.
2) Two horizontal slip directions (ψ) are determined for the two sets of best double couple parameters (λ, δ, ϕ) using the relation $\psi=\tan^{-1}(\tan\lambda\cos\delta)$ (Fig. 2a). The horizontal slip direction is derived from $\theta=\phi-\psi$.
3) The $\delta\theta$ value ($=\theta_{slip}-\theta_{model}$: Fig. 2b), which shows a smaller $|\delta\theta|$ value from two sets of best double couple parameters in the HCMT catalog, is determined as a realistic slip vector.

DEMETS (1993) constructed another plate motion model NUVEL-G, which does not use all slip vectors. The maximum difference between directions of relative motions obtained from NUVEL1 and NUVEL-G is less than 4°. Moreover, for most of the plate pairs, differences are less than 2° (see Table 3 in DEMETS, 1993). Therefore, NUVEL1 model is used as reference model of relative plate motion in this study.

4. Result

The relation between the slip vector deviations ($\delta\theta$) and seismic moment in 1977–1996 is shown in Fig. 3. Increase of scattering of $\delta\theta$ coincides with decrease of the seismic moment. It is estimated in Fig. 3 that a wide range distribution of $\delta\theta$ between

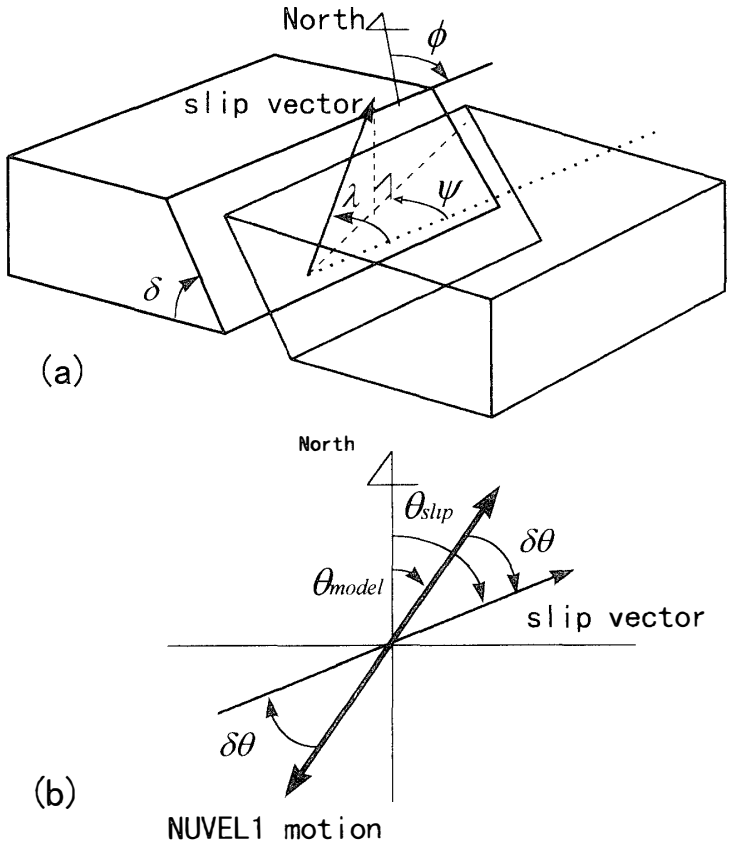

Fig. 2. (a) Spatial geometry of the fault plane and slip direction of the earthquake, ϕ is strike of fault, δ is dip of the fault, λ is rake angle, ψ is angle between strike and projected slip vector in the horizontal plane; (b) Definition of slip direction (θ_{slip}) and deviation ($\delta\theta$) of slip vector from prediction (θ_{model}) based on plate motion model (NUVEL1; DEMETS et al., 1990).

$-70°$ and $70°$ expresses random deformation uncorrelated with plate motion and/or random errors due to low S/N ratios of waveforms.

Figure 4 shows the relation between number of data and seismic moment used in this study and in NUVEL1 construction. DEMETS *et al.* (1990) mainly used the results of HCMT (1977–1987) without any selection criterion in terms of earthquake size to construct the NUVEL1 model. HCMT data from 1977 to 1996 are used in this study. The number of data used in this study is about 3 times larger than that used in NUVEL1 (1977–1987) (Fig. 4). Results for earthquakes with seismic moment larger than $10^{24.9}$ dyne·cm are used (144 events out of 693 events), because the scatter of distribution of $\delta\theta$s is larger for smaller seismic moment (Fig. 3). Moving averaged values of $\delta\theta$s and these standard deviations within a $10°$ longitude window for the data set of NUVEL1 (233 slip vectors are used for the circum-Antarctic region) are shown in Fig. 5a. Those selected by truncation are also shown in Fig. 5b. Moving averaged values are only determined, if number of values within a moving window is larger than 5. Selected 144 slip vectors whose seismic moments are larger than $10^{24.9}$ dyne·cm (Fig. 5b) show obvious reduction of the standard deviations (the mean reduction of average standard deviations is 58%) compared with those of the data set used in NUVEL1.

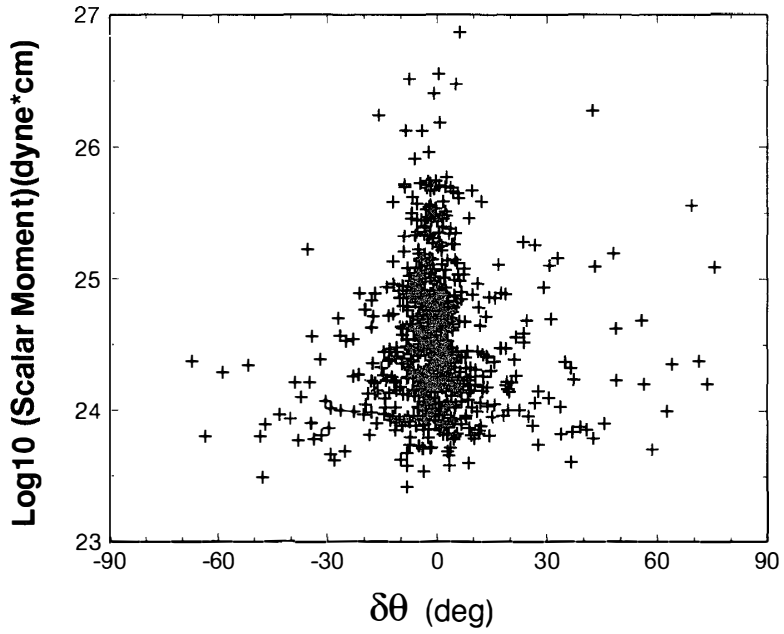

Fig. 3. Relation between $\delta\theta$s and seismic moments. Model predictions of plate motion are based on NUVEL1 (DeMets et al., 1993).

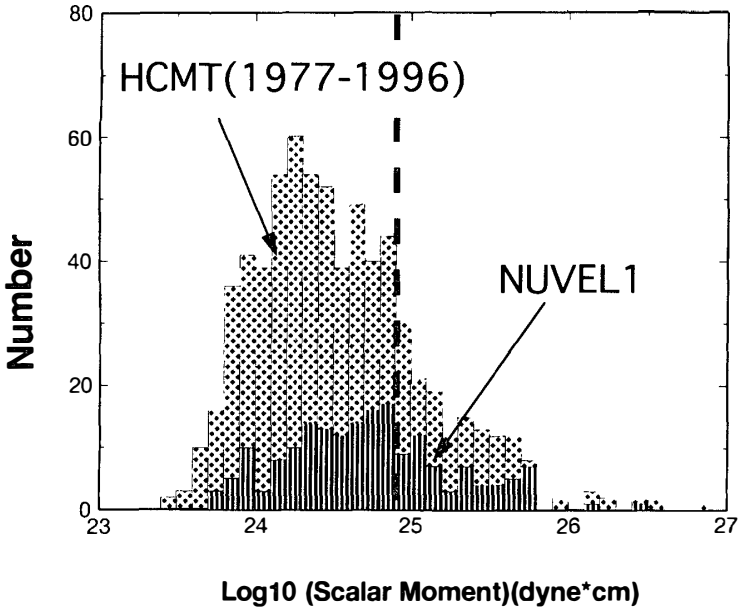

Fig. 4. Histogram of seismic moment for the data used in this study (1977–1996) and NUVEL1 (DeMets et al., 1990; 1977–1987) at the circum-Antarctic plate boundaries. Broken line is threshold of data selection (see text).

In the area of the PAC-ANT and the AUS-ANT boundaries, reductions of standard deviations of $\delta\theta$s are evident. However, at the SAM-ANT and AFR-ANT boundaries, reductions of standard deviations are not obtained. Deviations of $\delta\theta$s observed in the eastern part of the AUS-ANT boundary and the eastern part of the PAC-ANT boundary are clear. DeMets *et al.* (1988) has discussed counterclockwise

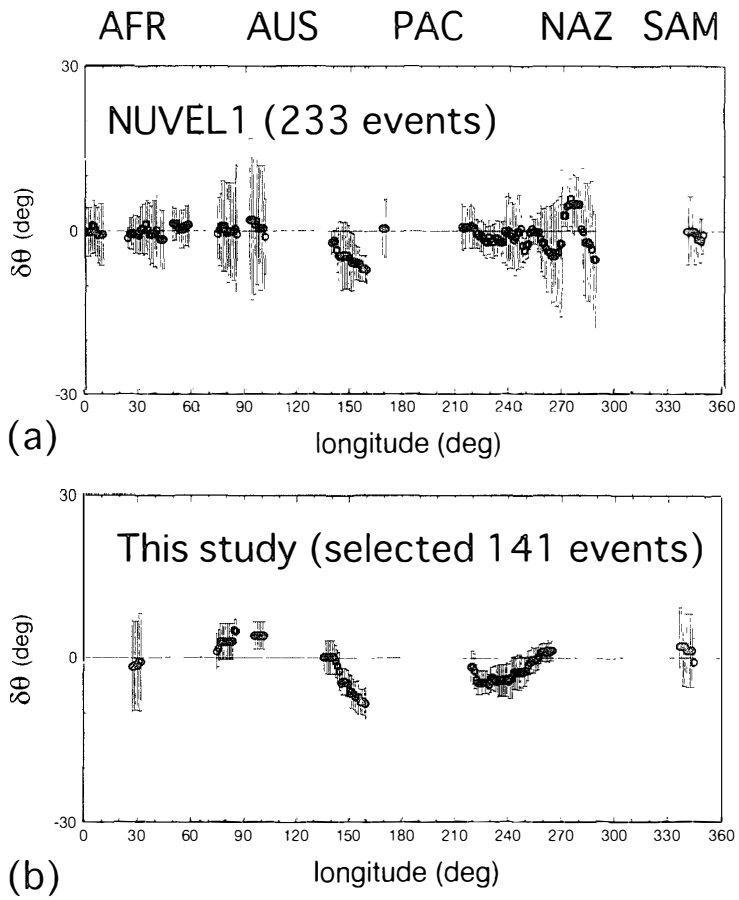

Fig. 5. Regional deviations of $\delta\theta$ values and their standard deviations. These are calculated as moving averages within a window of longitude which has 10° width. These are determined only if the number of data in the moving window is larger than 5. (a) NUVEL1 data set (233 events) without truncation, (b) data set of this study with truncation using threshold level of $10^{24.9}$ dyne·cm.

deviations (negative $\delta\theta$) up to 5° at the eastern end of the AUS-ANT region. Selected slip vectors show deviations greater than 5° in this study (Fig. 5b). Several degrees of slip vector deviations in the region of eastern end of the PAC-ANT boundary are discovered in this study, while no clear systematic deviations are detected in the NUVEL1 data set (Fig. 5a, b). In other regions, no systematic deviations are found, because of the large standard deviations.

5. Discussion

5.1. Reliability of the slip vector deviations

The standard deviations of moving averages of slip vector deviations ($\delta\theta$s) (Fig. 5b) are reduced to 3–5° at the eastern end of the AUS-ANT and the eastern part of the PAC-ANT boundaries (Fig. 5a) by using data whose seismic moments are larger than $10^{24.9}$ dyne·cm, although the reductions of standard deviations are not clear at the SAM-ANT and AFR-ANT boundaries. This implies that an estimate of systematic deviations larger than 3–5° is reliable at least near the eastern end of the AUS-ANT and

the eastern part of the PAC-ANT boundaries. HELFFRICH (1997) concludes that typical azimuthal resolution of the focal mechanism of shallow earthquakes is about 14° based on correlations among radiation patterns of three catalogs (HCMT, USGS, ERI) of centroid moment tensor solutions. However, the random deviations of focal mechanisms which depend on seismic moment were not considered in his study and ERI catalog shows weak correlation with other two catalogs (HCMT and USGS). Strong correlation between HCMT and USGS suggests that azimuthal resolution will be better than 14° just using HCMT and USGS. We believe that systematic deviations more than 5° are reliable by the truncation of the data whose seismic moments are less than $10^{24.9}$ dyne·cm at least in the eastern end of the AUS-ANT and the eastern part of the PAC-ANT boundaries. Azimuthal resolution using only HCMT and USGS should be determined in further analysis.

5.2. Dependence of slip vector deviations on spreading rate

Moving averaged values of $\delta\theta$s for the longitude window show large scatters or are not defined in regions of slow spreading rate (<4 cm/y: the SAM-ANT and the AFR-ANT boundaries), because of low seismicity and/or maximum seismic moment which depends on the spreading rate. Relations between $\delta\theta$s and seismic moments for slow and fast spreading rates are shown in Fig. 6, respectively. Random deviations of $\delta\theta$s are larger in regions of slow spreading rates, in contrast with those in the region of fast spreading rate. The maximum seismic moment depends on spreading rates (BURR and SOLOMON, 1978). Maximum seismic moment of the earthquake at transform faults are 10^{27} dyne·cm and 10^{28} dyne·cm for spreading rate of 6 cm/y and 2 cm/y, respectively (BURR and SOLOMON, 1978). The maximum seismic moment for slow spreading rate is approximately one order larger than that for a fast spreading rate. We used the constant threshold level ($10^{24.9}$ dyne·cm) for the determination of slip vector deviations. Higher threshold level should be used to reduce the effect of the random deviations and obtain good resolution of systematic deviations in the region of slow spreading rate. However, seismicity in a region of slow spreading rate is lower than that in a region of fast spreading. If a higher threshold level is applied in the a region of slow spreading rate, systematic deviations can not be determined by using current data set, because of small number of the data in the region of slow spreading rate.

In the following sections, causes of clear systematic deviations of slip vectors in the regions of fast spreading rates are discussed.

5.3. Possible causes of slip vector deviations from NUVEL1 predictions

Four causes are considered as the candidates of slip vector deviations at the eastern end of the AUS-ANT boundary and the eastern part of the PAC-ANT boundary. These are illustrated in Fig. 7a–d. The first is a slip vector deviation which depends on the sense of lateral faulting (DEMETS, 1993: Fig. 7a). The second is an unrecognized micro plate near the plate boundary (Fig. 7b). The third is relative motion between intraplate blocks in the Antarctic plate (Fig. 7c). The fourth is deformation around plate boundaries, which is related to plate boundary reorganization (Fig. 7d). Each possibility is discussed in the following sections.

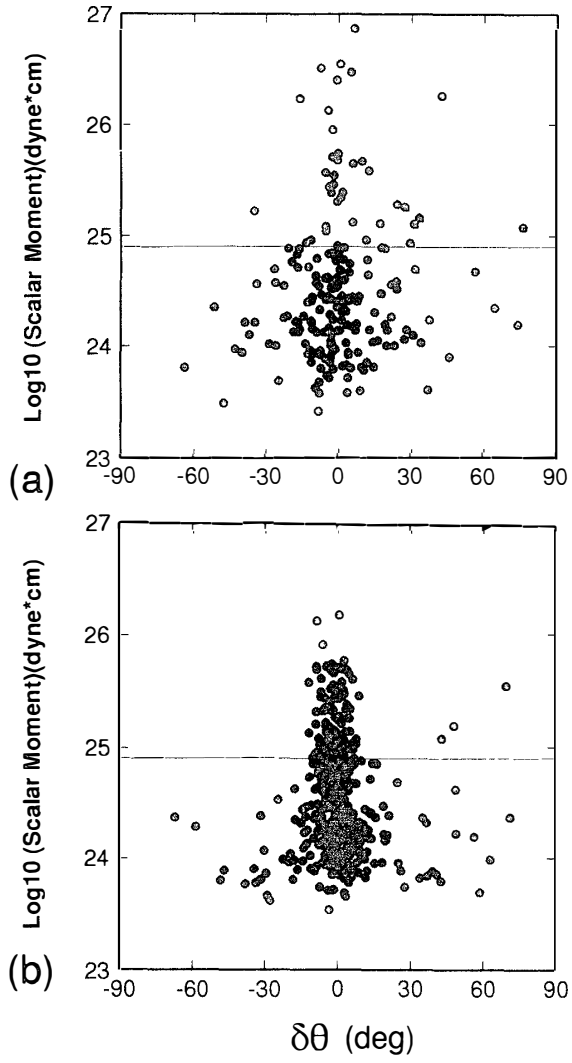

Fig. 6. Slip vector deviations and their seismic moment, (a) in the region of spreading rates slower than 4 cm/y, (b) in the region of spreading rate faster than 4 cm/y.

5.4. Possibility of the transpressional deformation with thrust component at transform earthquake

One of the possible causes for systematic deviations is the sense of lateral faulting. DEMETS (1993) shows that the sense of lateral faulting correlates with the sense of slip vector deviations. Positive and negative $\delta\theta$s are expected for right lateral and left lateral transform faults, respectively (Fig. 7a). In our study, clear deviations of $\delta\theta$s appeared in regions of left lateral faulting and show negative $\delta\theta$ (Fig. 8a). This result agrees with the correlation of senses between lateral faulting and $\delta\theta$ of slip vector shown in DEMETS (1993).

Lateral faulting with thrust a component will satisfy DEMETS's consequence. Another essential parameter of the direction of relative motion is the strike of the transform fault. If earthquakes at transform faults show pure strike slips, both strike and slip directions agree with each other. But strikes of earthquake faults show similar deviation patterns of slip vectors for both at the eastern end of the AUS-ANT and in the

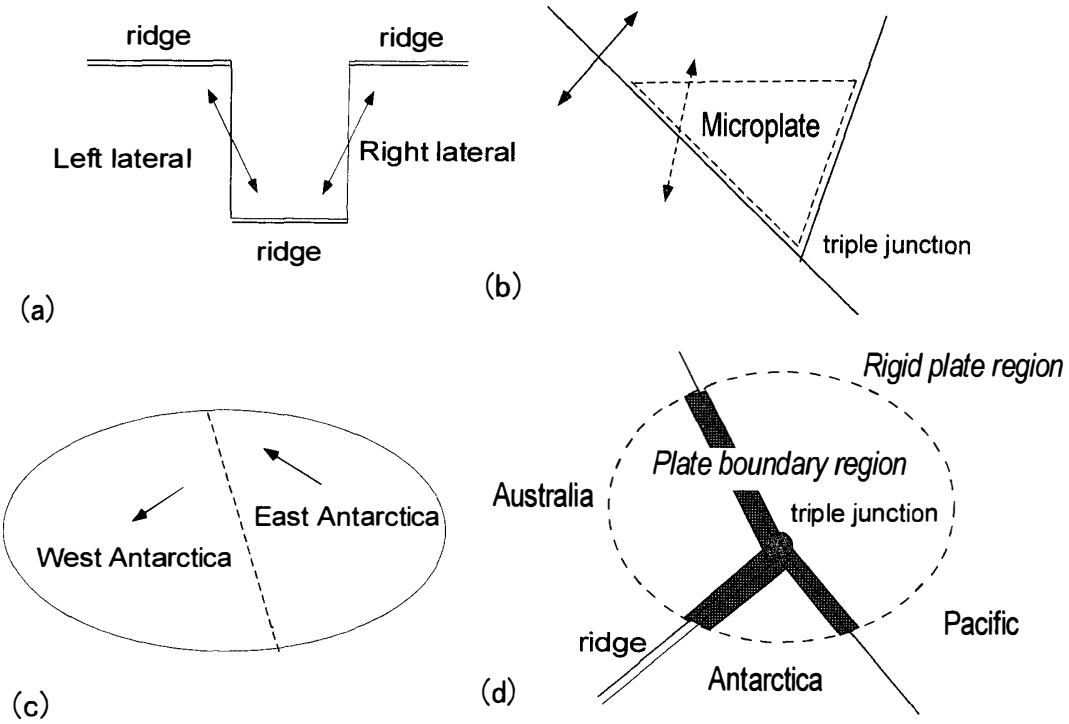

Fig. 7. Possible causes of slip vector deviations ($\delta\theta$). (a) Transpressional deformation with thrust component of transform fault earthquakes; (b) presence of unrecognized microplates; (c) decoupled motion between East and West Antarctica; (d) plate boundary reorganization related to triple junction. Hatched regions are affected by reorganization of plate boundaries in addition to rigid relative motion.

eastern part of the PAC-ANT in our study (Fig. 8b). This suggests that slip directions coincide with strikes in these regions. These earthquakes show typical pure strike slips without any thrust components. Therefore, the strike slips with thrust components are not the cause of systematic deviations of slip vectors.

5.5. *Possibility of unrecognized microplates*

Slow relative motion between unrecognized microplates and the major plate is one of the possible causes of slip vector deviations (Fig. 7b). DEMETS *et al.* (1988) recognized systematic deviations of slip vectors at the eastern end of the AUS-ANT boundary from their best fit model and RM2 (MINSTER and JORDAN, 1978). They discussed the possibility of a microplate in the Australian plate between 140° and 160°E near the triple junction. Negative $\delta\theta$s (counterclockwise slip vector deviations) are consistent with E-W and ENE-WSW motion of hypothetical microplates relative to the rest of the Australian plate (in Fig. 9: motion plotted as an arrow in the AUS plate). A slip direction of an intraplate event on the hypothetical microplate boundary (broken line in Fig. 9) is inconsistent with the predicted direction based on microplate hypothesis (see Fig. 19 in DEMETS *et al.*, 1988).

A large intraplate earthquake took place in the Antarctic plate on 25 March 1998 (lat: 62.876°S; lon: 149.712°E; depth: 10km, M_w=8.1, USGS Balleny Island region; Fig. 9). A similar microplate hypothesis could be considered for the Antarctic plate.

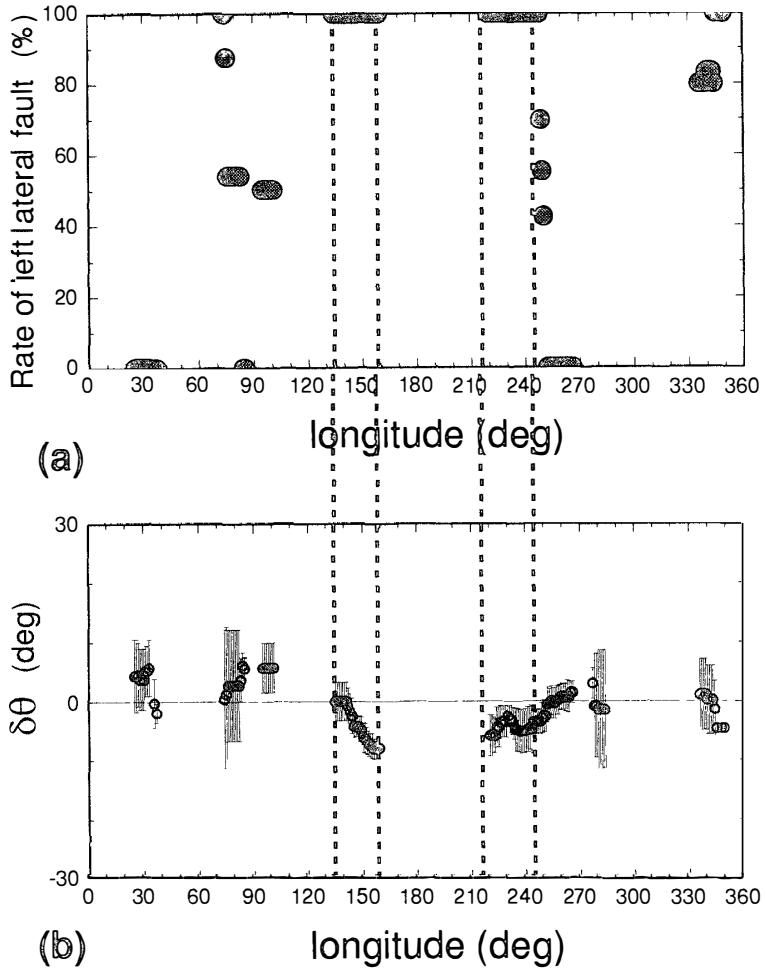

Fig. 8. (a) Rates of left lateral transform faults within 10° longitude ranges based on rake angles of focal mechanisms, (b) Strike directions of transform faults are also derived for selected dataset of HCMT.

Motion of several millimeters per year toward the ENE relative to other parts of Antarctica (arrow in the ANT plate in Fig. 9) is estimated from observed $\delta\theta$s. If we assume no active drag of the sub-lithosphere, hypothetical relative motion forms a compressional axis along the NW-SE or NNW-SSE direction (NE-SW or ENE-WSW extension) within the ANT plate. However, the preliminary mechanism of the Balleny Island event shows an ENE-WSW or NE-SW compression axis (USGS QED report, 1998; KIKUCHI and YAMANAKA, 1998) which is nearly perpendicular to the predicted direction of stress based on deviated $\delta\theta$s at the plate boundary. Possible slip vector directions are also inconsistent with that predicted from negative $\delta\theta$s at plate boundary, regardless of ambiguity between the real fault and auxiliary plane. These inconsistencies of stress and slip directions on the hypothetical microplate boundary suggest that unrecognized microplate is not the cause of systematic slip vector deviations of the plate boundary.

In the eastern part of the PAC-ANT boundary, there is no seismicity in the HCMT catalog which suggests that a microplate boundary have been found, although a Juan

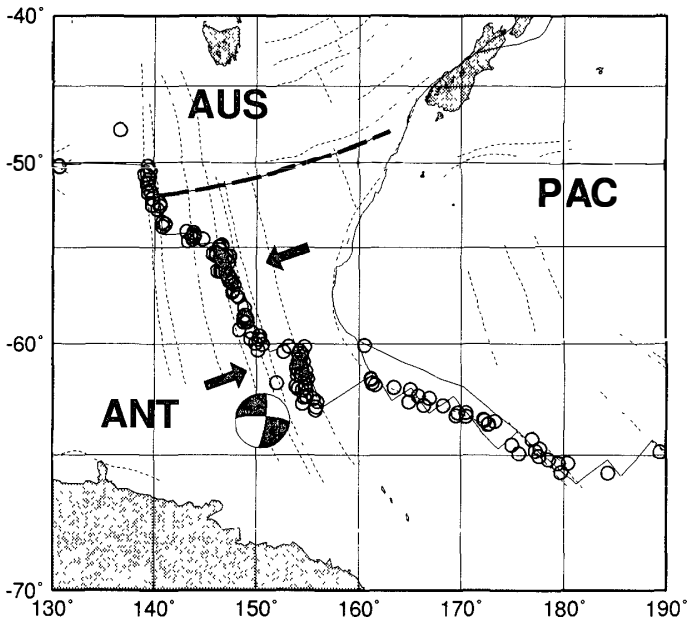

Fig. 9. Tectonic map of the microplate around the eastern end of the AUS-ANT boundary. The broken line is the hypothetical microplate boundary assumed in DEMETS *et al. (1998). Predicted motions about several mm/y toward WSW and ENE directions in the AUS and ANT plates, respectively. Focal mechanism of Balleny Island event on 25 March 1998 (lat: 62.876°S; lon: 149.712°E; depth: 10 km; M_w=8.1, USGS) is drawn on the epicenter.*

Fernandez micro plate is suggested at the PAC-ANT-NAZ triple junction. Thus a microplate origin of slip vector deviations is not possible for the eastern part of the PAC-ANT boundary.

5.6. *Possibility of decoupled deformation between East and West Antarctica*

Relative motion between East and West Antarctica has been suggested by a reconstruction study (MOLNAR *et al.*, 1975). If such decoupled motion between East and West Antarctica has continued until the present, it should also have created the deviations of slip vectors from predictions of plate motion model. YAMADA *et al.* (1998) analyzed 5 GPS stations on the Antarctic plate by a precise point positioning technique. They obtained Euler rotation parameters of the Antarctic plate relative to International Terrestrial Reference Frame 94 (ITRF94). Figure 10 shows residual motions, which are formed by subtracting fitted rigid plate motions from observed rates at 5 GPS stations. Although these results are preliminary, motion at McMurdo show largest in these 5 stations, and the direction of residual motion at McMurdo is ENE. If this reflects large scale motion of West Antarctica, such motion could explain observed slip vector deviations of about 5°. Although, continuous monitoring is required for eastward motion of McMurdo and other stations in West Antarctica, relative motion between East and West Antarctica is one of the possible causes of slip vector deviations at the eastern end of the AUS-ANT boundary. However extended hypothetical boundary between East and West Antarctica in the ocean should be located near the epicenter of the Balleny Island event (Fig. 9). If we assume that the epicenter

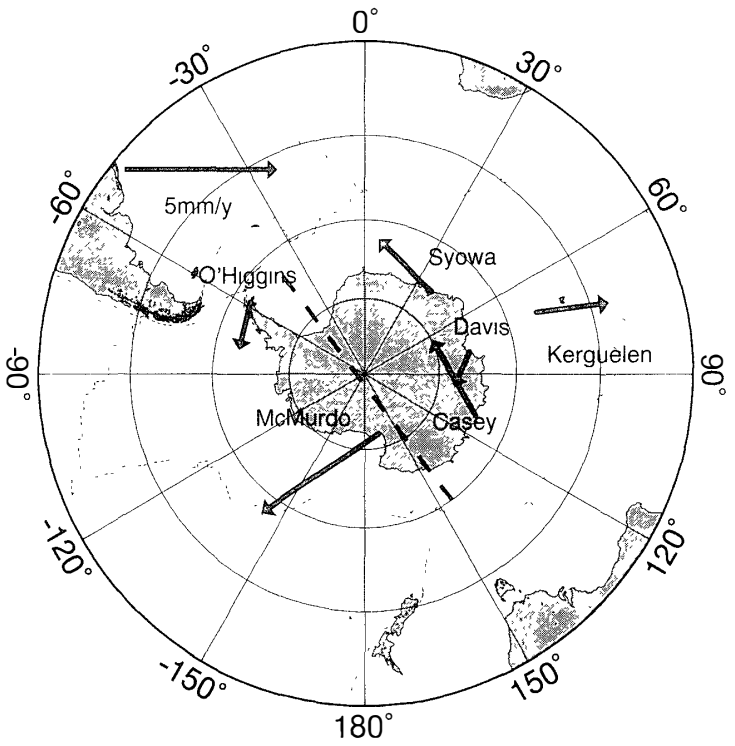

Fig. 10. Residual motions obtained by subtracting fitted rigid plate motions in the Antarctic plate (Reproduced from YAMADA et al., 1998). Fitted rotation parameters of the Antarctic plate relative to the ITRF94 reference frame are as follows; lat: 62.7° E; lon: 128.4° W; angular velocity: 0.22°/my. The broken line shows Transantarctic Mountains, which bounds between East and West Antarctica.

is located on the boundary, deformation of eastward motion is also inconsistent with the focal mechanism of before Balleny Island event.

The eastern region of the PAC-ANT plate boundary is far from the geodetic stations. Therefore the possibility of motion between East and West Antarctica cannot be discussed in the eastern region of the PAC-ANT boundary.

5.7. Comparison with estimation of relative motions based on geodetic measurements

Deviations of earthquake slip vectors are compared with those predicted by the Euler poles using geodetic measurements (LARSON *et al.* 1997). Relative motions by GPS for the AFR-ANT, SAM-ANT, and NAZ-ANT show that error estimations of pole locations are larger than 10°. Results of GPS measurements in these regions are not useful in this discussion, because there are large errors as same as those of slip vectors. We can compare results of slip vectors at the AUS-ANT and the PAC-ANT boundary with poles estimated by GPS, because of small errors of pole location within 4.4°.

The rotation pole of the AUS-ANT motion was estimated by GPS apart several degrees southeastward from that of NUVEL1's (Fig. 11a). Slip vectors at the eastern end of the AUS-ANT boundaries show negative $\delta\theta$ values. Meridian great circles, which are perpendicular to slip vectors at epicenters, are drawn in Fig. 11a. Great circles from slip vectors at the eastern end of the AUS-ANT boundary (140°-160° E,

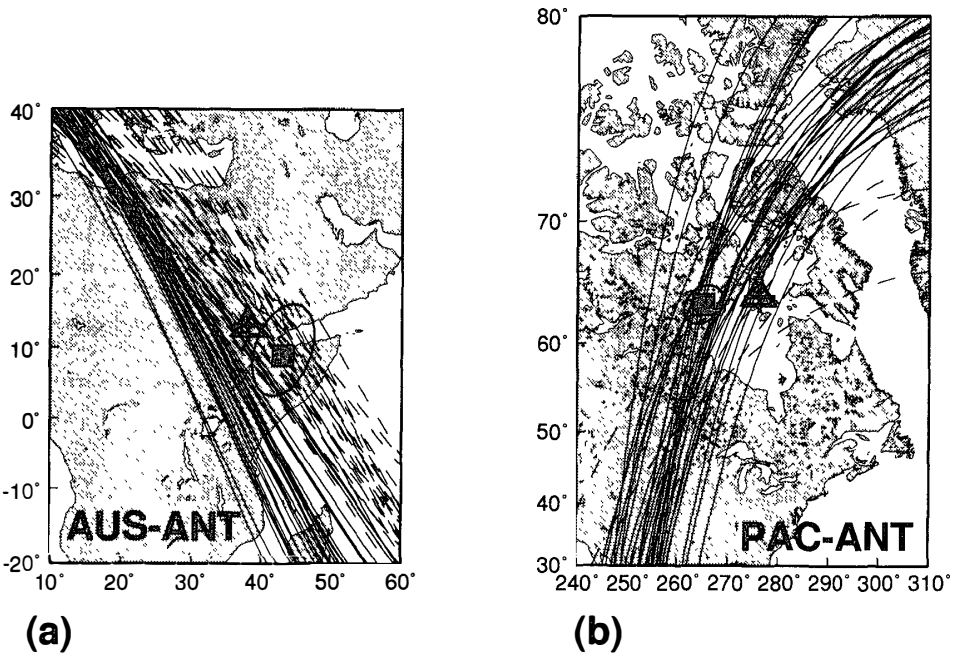

Fig. 11. Pole locations of the relative plate motions and meridian great circles which are perpendicular to slip vectors at epicenters. Crosses are pole locations by NUVEL1; solid squares are pole locations based on the GPS (LARSON et al., 1997). Open triangles are locations of NUVEL-G (DEMETS et al., 1993), in which all slip vectors are excluded. Ellipses show error estimation for geodetic pole locations. (a) AUS-ANT case, (b) PAC-ANT case.

solid line in Fig. 11a) apart more than several degrees from both poles by NUVEL1 and GPS. These great circles clearly apart from distribution of other part of the AUS-ANT boundaries (dotted lines in Fig. 11a). These data suggest decoupled deformation of the region from the large part of the plate. However, block motions due to the microplate boundary is also inconsistent with observation discussed above. Deformation related to plate boundary reorganization near the triple junction is a possible cause of slip vector deviations.

In the eastern part of the PAC-ANT boundary, meridian great circles of slip vectors pass between the NUVEL1 pole and the geodetic pole (Fig. 11b). Meridian great circles from slip vectors are more scattered than those in the AUS-ANT case. Misfits of motions determined by VLBI from best fitted plate motions in the PAC also show larger residuals than those of other plates (ARGUS and GORDON, 1996). The 1) mislocation of pole estimation, and/or 2) reorganization of plate boundary are possible causes of systematic deviations of slip vectors. However, the causes has not been identified yet. Denser observation of satellite geodesy and analysis of strain localization within PAC-ANT plates are required to answer the causes of slip vector deviations at the PAC-ANT boundary.

6. Conclusions

Clear systematic deviations of slip vectors from the predicted directions by

NUVEL1 are found around the eastern end of the AUS-ANT and the PAC-ANT plate boundaries from earthquakes with a seismic moment between $10^{24.9}$ and $10^{26.8}$ dyne·cm. At the eastern end of the AUS-ANT boundary, detected systematic deviations of slip vectors from NUVEL1 cannot be explained by the rotational pole based on geodetic study. A microplate hypothesis or relative motion between East and West Antarctica does not explain stress and/or slip directions of recent large intraplate earthquakes. The deviations of slip vectors are most likely caused by evolution of the plate boundaries. In contrast, causes of systematic deviations of slip vectors for the eastern part of the PAC-ANT boundary have not been identified in this study. Further observations are necessary to determine the cause of systematic deviations of slip vectors for the eastern part of the PAC-ANT.

Acknowledgments

We thank F. TAJIMA and Y. HARADA for careful reviews. T. SENO critically read the manuscript at an early stage.

References

ARGUS, D.F. and GORDON, R. (1996): Test of the rigid plate hypothesis and bounds on plate rigidity using geodetic data from very long baseline interferometry. J. Geophys. Res., **101**, 13555–13572.

ARGUS, D.F. and HEFIN, M.B. (1995): Plate motion and crustal deformation estimated with geodetic data from the Global Positioning System. Geophys. Res. Lett., **22**, 1973–1976.

BURR, N.C. and SOLOMON, S.C. (1978): The relationship of source parameters of oceanic transform earthquakes to plate velocity and transform length. J. Geophys. Res., **83**, 1193–1205.

CHASE, C.G. (1978): Plate kinematics: The Americas, east Africa, and the rest of the world. Earth Planet. Sci. Lett., **37**, 355–368.

DALZIEL, I.W.D. (1992): Antarctica: A tail of two supercontinents? Ann. Rev. Earth Planet. Sci., **20**, 501–526.

DEMETS, C. (1993): Earthquake slip vectors and estimates of present-day plate motions. J. Geophys. Res., **98**, 6703–6714.

DEMETS, C., GORDON, R.G. and ARGUS, D. (1988): Intraplate deformation and closure of the Australia-Antarctica-Africa plate circuit. J. Geophys. Res., **93**, 11877–11897.

DEMETS, C., GORDON, R.G., ARGUS, D.F. and STEIN, S. (1990): Current plate motions. Geophys. J. Int., **101**, 425–478.

DZIEWONSKI, A.M. and WOODHOUSE, J.H. (1983): An experiment in the systematic study of global seismicity: Centroid-moment tensor solutions for 201 moderate and large earthquakes of 1981. J. Geophys. Res., **88**, 3247–3271.

DZIEWONSKI, A., CHOU, T.-A. and WOODHOUSE, J.H. (1981): Determination of earthquake source parameters from waveform data for studies of global and regional seismicity. J. Geophys. Res., **86**, 2825–2852.

HEKI, K. (1996): Horizontal and vertical crustal movements from three dimensional very long baseline interferometry kinematic reference frame: Implications for the reversal timescale revision. J. Geophys. Res., **101**, 3187–3198.

HELFFRICH, G.R. (1997): How good are routinely determined focal mechanisms? Empirical statistics based on a comparison of Harvard, USGS and ERI moment tensors. Geophys. J. Int., **131**, 741–750.

KIKUCHI, M. and YAMANAKA, Y. (1998): EIC Seismology Note, No. 41, 3 p.

LARSON, K.M., FREYMUELLER, J.T. and PHILIPSEN, S. (1997): Global plate velocities from the Global Positioning System. J. Geophys. Res., **102**, 9961–9982.

MINSTER, J.B. and JORDAN, T.H. (1978): Present-day plate motions. J. Geophys. Res., **83**, 5331–5354.

MINSTER, J.B., JORDAN, T.H., MOLNAR, P. and HAINES, E. (1974): Numerical modeling of instantaneous

plate tectonics. Geophys. J. R. Astron. Soc., **36**, 541–576.

MOLNAR, P., ATWATER, T., MAMMERICKX, J. and SMITH, S.M. (1975): Magnetic anomalies, bathemetry and the tectonic evolution of the Pacific since the late Cretaceous. Geophys. J. R. Astron. Soc., **40**, 383–420.

PELAYO, A.M. and WIENS, D.A. (1989): Seismotectonics and relative plate motion in the Scotia Sea region. J. Geophys. Res., **94**, 7293–7320.

ROULT, G., ROULAND, D. and MONTAGNER, J.P. (1994): Antarctica II: Upper-mantle structure from velocities and anisotropy. Phys. Earth Planet. Inter., **84**, 33–57.

YAMADA, A., MARUYAMA, K., OOTAKI, O., ITABASHI, A., HATANAKA, Y., MIYAZAKI, S., NEGISHI, H., HIGASHI, T., NOGI, Y., KANAO, M. and DOI, K. (1998): Analysis of GPS data at Syowa Station and IGS tracking stations. Polar Geosci., **11**, 1–8.

(Received March 23, 1998; Revised manuscript accepted June 16, 1998)